Title

CARD9+ microglia promote antifungal immunity via IL-1β- and CXCL1-mediated neutrophil recruitment.

Authors

Drummond, Rebecca A
Swamydas, Muthulekha
Oikonomou, Vasileios
et al.

CARD9+ Microglia Promote Antifungal Immunity via IL-1β and CXCL1-mediated Neutrophil Recruitment

Rebecca A. Drummond[1],[*],[†], Muthulekha Swamydas[1],[#], Vasileios Oikonomou[1],[#], Bing Zhai[2],[#], Ivy M. Dambuza[3], Brian C. Schaefer[4], Andrea C. Bohrer[5], Katrin D. Mayer-Barber[5], Sergio A. Lira[6], Yoichiro Iwakura[7], Scott G. Filler[8], Gordon D. Brown[3], Bernhard Hube[9],[10], Julian R. Naglik[11], Tobias M. Hohl[2], and Michail S. Lionakis[1],[*]

[1]Fungal Pathogenesis Section, Laboratory of Clinical Immunology and Microbiology (LCIM), National Institute of Allergy & Infectious Diseases (NIAID), National Institutes of Health (NIH), Bethesda, MD, USA

[2]Infectious Disease Service, Department of Medicine, Memorial Sloan-Kettering Cancer Center, New York, NY, USA

[3]Medical Research Council Centre for Medical Mycology at the University of Aberdeen, Aberdeen Fungal Group, Institute of Medical Sciences, University of Aberdeen, Aberdeen AB25 2ZD, UK

[4]Department of Microbiology and Immunology, Uniformed Services University, Bethesda, MD 20814

[5]Inflammation and Innate Immunity Unit, LCIM, NIAID, NIH, Bethesda, MD, USA

[6]Immunology Institute, Icahn School of Medicine at Mount Sinai, New York, NY 10029, USA

[7]Research Institute for Biomedical Sciences, Tokyo University of Science, Chiba, Japan

[8]Division of Infectious Diseases, Department of Medicine, Los Angeles Biomedical Research Institute at Harbor—UCLA, Torrance, CA, 90502

[9]Department of Microbial Pathogenicity Mechanisms; Leibniz Institute for Natural Product Research and Infection Biology; Hans Knöll Institute Jena; Jena, Germany

[10]Friedrich Schiller University, Jena, Germany

[11]Centre for Host-Microbiome Interactions, Faculty of Dentistry, Oral and Craniofacial Sciences, King's College London, London, United Kingdom

[*]Correspondence: r.drummond@bham.ac.uk; lionakism@niaid.nih.gov.
[†]Current address: Institute of Immunology & Immunotherapy, Institute of Microbiology & Infection, University of Birmingham, Birmingham B15 2TT, UK
[#]These authors contributed equally to this work

Abstract

The C-type lectin receptor–Syk adaptor CARD9 facilitates protective antifungal immunity within the central nervous system (CNS), as human CARD9-deficiency causes fungal-specific CNS-targeted infection susceptibility. CARD9 promotes neutrophil recruitment to the fungal-infected CNS, which mediates fungal clearance. Here, we investigated host and pathogen factors that promote protective neutrophil recruitment during *Candida albicans* CNS invasion. IL-1β was essential for CNS antifungal immunity by driving CXCL1 production, which recruited CXCR2-expressing neutrophils. Neutrophil-recruiting IL-1β and CXCL1 production was induced in microglia by the fungal-secreted toxin Candidalysin, in a p38-cFos-dependent manner. Importantly, microglia relied on CARD9 for production of IL-1β, via both *Il1b* transcriptional regulation and inflammasome activation, and of CXCL1 in the fungal-infected CNS. Microglia-specific *Card9* deletion impaired IL-1β and CXCL1 production and neutrophil recruitment, and increased CNS fungal proliferation. Taken together, an intricate network of host-pathogen interactions promotes CNS antifungal immunity, which is impaired in human CARD9-deficiency leading to CNS fungal disease.

Introduction

The CNS is invaded by microorganisms during systemic infections, yet the mechanisms of CNS-specific anti-microbial immunity remain poorly-understood. This is particularly true for CNS fungal infections, which present unmet diagnostic and treatment challenges, leading to unacceptably high mortality rates (>50%)[1]. Fungal CNS invasion is enhanced by fungal-specific risk factors, including HIV infection, neutropenia, corticosteroid use, and Bruton's tyrosine kinase inhibition[1]. However, the most striking human risk factor for selective CNS fungal infection susceptibility is inherited deficiency of the C-type lectin receptor (CLR)–Syk adaptor CARD9.

CARD9 relays fungal-sensing signals downstream of the CLR superfamily of pattern recognition receptors, including Dectin-1, Dectin-2, Dectin-3 and Mincle. Syk kinase is recruited to phosphorylated ITAM sequences of CLRs or their signaling partner FcRγ to form the CARD9-BCL10-MALT1 signalosome, which activates downstream effectors including NFκB, NLRP3 inflammasome and MAPK signaling[2].

CARD9-deficient patients manifest fungal-specific infection susceptibility, predominantly in the CNS by *Candida albicans*[2-4]. We previously showed that CARD9-deficiency in humans and mice confers a fungal- and brain-specific defect in neutrophil recruitment, which is detrimental for control of CNS fungal invasion[5]. However, the CNS cellular and molecular cues that promote protective neutrophil recruitment during *C. albicans* invasion and their dependence on CARD9 *in vivo* remain unknown.

Herein, we systematically investigated host and pathogen factors that promote protective neutrophil influx into the *C. albicans*-infected CNS to better understand the pathogenesis of human CARD9-deficiency. We uncover an intricate pathway by which the *C. albicans*-secreted toxin Candidalysin engages microglia to produce IL-1β and CXCL1 for protective recruitment of CXCR2-expressing neutrophils. Importantly, microglial IL-1β and CXCL1

production depends on CARD9 and specific deletion of microglial CARD9 impairs neutrophil recruitment to the *C. albicans*-infected CNS. Collectively, our data unveil complex host-pathogen interactions that recruit protective neutrophils during fungal CNS invasion and reveal the mechanism that underlies CNS fungal susceptibility in CARD9-deficiency.

Results

CLR Functional Redundancy during Fungal CNS Invasion

As previously shown, CARD9 is essential for protective CNS immunity against *C. albicans*, principally through promoting early neutrophil recruitment (Fig. 1a). We first investigated the relative contribution of CARD9-coupled CLRs, which are expressed by brain-resident microglia (Supplementary Fig. 1), in mediating this protective neutrophil recruitment. We infected mice deficient in Dectin-1 ($Clec7a^{-/-}$), Dectin-2 ($Clec4n^{-/-}$), Dectin-3 ($Clec4d^{-/-}$) and Mincle ($Clec4e^{-/-}$) and measured brain neutrophil accumulation at 24 h post-infection (Supplementary Fig. 2). We chose this time-point since it is the peak of the neutrophil response in wild-type animals and neutrophil depletion at this time-point increases susceptibility to brain fungal invasion[5].

Animals individually deficient in CARD9-coupled CLRs recruited neutrophils to the infected brain normally (Fig. 1b). Despite this, we observed increases in fungal brain burdens at 72 h post-infection in mice deficient in Dectin-1 or Dectin-2 but not Dectin-3 or Mincle (Fig. 1c), suggesting that Dectin-1 and Dectin-2 employ neutrophil recruitment-independent mechanisms to protect against brain fungal proliferation. Indeed, brain-infiltrating neutrophils from Dectin-1– and Dectin-2-deficient animals exhibited reduced fungal phagocytosis (Supplementary Fig. 3), consistent with prior findings[6].

To activate CARD9-dependent signaling, phosphorylation occurs on the ITAM sequence within the intracellular tail of Dectin-1 or FcRγ, which Dectin-2, Dectin-3 and Mincle associate with. Therefore, we assessed whether deletion of all four CLRs affected the neutrophil response in the infected brain. We used mice doubly-deficient in Dectin-1 and FcRγ ($Clec7a^{-/-}Fcerg1^{-/-}$) and found that loss of both Dectin-1 and the FcRγ-coupled CLRs phenocopied Card9-deficiency with significantly decreased neutrophil recruitment and corresponding increased brain fungal burdens (Fig. 1b,c). Taken together, CARD9-coupled CLRs functionally compensate to mediate neutrophil recruitment-dependent protection against *C. albicans* CNS invasion.

MALT1 is Required for Defense against CNS Candidiasis

The CARD9-MALT1-BCL10 signalosome is necessary for transducing fungal-sensing intracellular signals. Human deficiencies of MALT1 or BCL10 cause defective innate and adaptive immune responses, and many of these patients die in childhood from bacterial and viral infections[2]. Human MALT1-deficiency additionally manifests with mucosal candidiasis, suggesting that antifungal immunity is impaired in these patients. However, whether MALT1-deficiency also predisposes to brain-targeted candidiasis is unknown. To test this, we infected Malt1-deficient mice and assessed control of CNS *C. albicans* growth.

Malt1^{-/-} animals recruited neutrophils to the brain similarly to wild-type, however these animals exhibited uncontrolled brain fungal growth at 72 h post-infection (Fig. 1d). Therefore, MALT1 is critical for protective CNS immunity against *C. albicans*; however, the MALT1-dependent protective mechanisms operating in this tissue are independent of neutrophil recruitment, unlike CARD9.

Candida Drives CNS Neutrophil Influx via IL-1β and CXCL1

To determine the local cues that recruit protective neutrophils in the infected CNS, we examined key cytokine and chemokine circuits using gene-deficient mice. We first infected IL-1 receptor (IL-1R)–deficient mice, because production of IL-1β by human peripheral blood mononuclear cells upon fungal stimulation is CARD9-dependent[5,7], and because IL-1R was previously shown to recruit neutrophils to fungal-infected mucosal tissues[8,9], and to the bacterial-infected brain[10]. Upon *C. albicans* challenge, IL-1R–deficient mice phenocopied Card9-deficient mice, with a loss of early brain neutrophil recruitment and accompanying increased fungal brain burdens (Fig. 2a,b). Consistent with this, loss of the IL-1R signaling adaptor MyD88 caused similar defects in neutrophil recruitment and control of fungal proliferation in the infected brain (Fig. 2a,b).

We next assessed which IL-1R ligands were important for driving CNS protection by infecting mice deficient in IL-1α, IL-1β or both. Mice lacking IL-1α had a small reduction in neutrophil numbers and a slight increase in fungal brain burden at 24 h post-infection (Fig. 2a,b). However, the lack of IL-1α was compensated by IL-1β, since *Il1a*^{-/-} animals recovered and controlled fungal brain infection similar to wild-type by 72 h post-infection (Fig. 2b). In keeping with the critical contribution of IL-1β, mice deficient in IL-1β, or both IL-1α–IL-1β, exhibited significantly reduced neutrophil accumulation and were highly susceptible for fungal brain invasion (Fig. 2a,b). Therefore, IL-1β is a critical mediator of neutrophil recruitment to promote control of *C. albicans* brain infection.

Downstream of IL-1R, local chemotactic mediators recruit immune cells to infected tissues. Previously, we showed that the CNS-neutropenia observed in mouse and human CARD9-deficiency is not caused by neutrophil-intrinsic chemotaxis defects[5], but by insufficient local production of soluble chemotactic mediators. However, which among the several chemoattractants and their receptors recruit(s) protective neutrophils to the *C. albicans*-infected CNS is unknown.

CARD9 was shown to drive production of the CXCR2 ligands CXCL1 and CXCL2 during inflammatory arthritis[11] and murine subcutaneous phaeohyphomycosis[12]. During systemic *C. albicans* infection, CCR1 drives renal neutrophil accumulation and immune-related kidney destruction[13], the leukotriene B4 (LTB$_4$) receptor LTB4R1 promotes detrimental pulmonary neutrophil accumulation[14], and CXCR1 mediates neutrophil-dependent fungal killing in the kidney[15]. However, the role of these receptors in CNS anti-*Candida* immunity is unknown, while CXCR2 and the fMet-Leu-Phe (fMLP) receptor FPR1 have not been examined in anti-*Candida* defense.

To test the relative dependence on these major neutrophil-targeted chemoattractant receptors in protecting the fungal-infected brain, we infected mice deficient in CCR1, CXCR1,

CXCR2, LTB4R1 or FPR1 and measured neutrophil recruitment and fungal brain burdens. We found no involvement of the CCL3–CCR1, CXCL5–CXCR1, LTB4–LTB4R1 or fMLP–FPR1 axes in controlling fungal brain infection, in line with normal early neutrophil recruitment in infected *Ccr1*^{−/−}, *Cxcr1*^{−/−}, *Ltb4r1*^{−/−} and *Fpr1*^{−/−} animals (Fig. 2c,d **and** Supplementary Fig. 4). In contrast, CXCR2-deficient mice had significantly reduced neutrophil accumulation and corresponding significantly increased fungal brain growth (Fig. 2c,d). These data demonstrate the importance of the CXCR2 axis in neutrophil-mediated protection against *C. albicans* brain infection.

Next, we wondered which CXCR2 ligand may recruit protective neutrophils to the fungal-infected brain. We infected *Cxcl1*^{−/−} mice that lack expression of the potent neutrophil chemokine CXCL1. Notably, these animals had decreased neutrophil recruitment to the brain post-infection and exhibited a similar CNS invasion susceptibility phenotype to *Cxcr2*^{−/−} mice (Fig. 2c,d). Therefore, the CXCL1–CXCR2 chemokine axis is critical for protection against *C. albicans* brain invasion by recruiting protective neutrophils. Importantly, this data indicates that the reduced CXCL1 in the human CARD9-deficient *C. albicans*-infected cerebrospinal fluid is biologically relevant and significant[5].

IL-1β Activates CXCL1 in the Fungal-Infected Brain

Since both IL-1β and CXCL1 were required for protection, we investigated whether their activation in the infected brain was simultaneous or sequential. We measured IL-1β and CXCL1 in brain homogenates at 24 h post-infection in animals lacking these inflammatory mediators. We found no defect in IL-1β levels in CXCL1-deficient infected brains; however, we discovered a significant defect in CXCL1 production in the absence of IL-1β (Fig. 3a). To define the IL-1β–dependent brain cellular sources of CXCL1, we infected wild-type and IL-1β–deficient mice and used intracellular flow cytometry. CXCL1 and pro-IL-1β were produced by multiple myeloid phagocytes in the fungal-infected brain, including resident microglia, the most numerous immune cells in the brain, recruited Ly6C^{hi} monocytes which have been implicated in controlling *C. albicans* CNS invasion[16], and neutrophils themselves (Fig. 3b). Interestingly, *Il1b*^{−/−} microglia recovered from *C albicans*-infected brains had a profound defect in CXCL1 production, exhibiting significant reductions under every *ex vivo* restimulation condition tested (Fig. 3c). Ly6C^{hi} monocytes isolated from *Il1b*^{−/−} *C. albicans*-infected brains produced less CXCL1 when restimulated *ex vivo* with LPS, with no differences detected under non-stimulated or zymosan-stimulated conditions. Neutrophil production of CXCL1 did not differ between the two mouse groups (Fig. 3c). Therefore, IL-1β is required for subsequent CXCL1 production from resident microglia and recruited monocytes, which in turn recruits CXCR2-expressing neutrophils to the fungal-infected brain.

Candidalysin is a Fungal Avirulence Factor in the Brain

Use of genetically-deficient mice allowed us to map the host pathway promoting protection against *C. albicans* brain infection, in which IL-1β–IL-1R–MyD88 signaling activates CXCL1 production by resident microglia and recruited monocytes to mobilize neutrophils into the CNS. To identify the pathogen-associated factors that induce this protective host

pathway, we infected animals with *C. albicans* strains lacking known virulence factors and assessed neutrophil recruitment and IL-1β and CXCL1 production in the infected brain.

C. albicans hyphae are the predominant CNS-invasive morphological forms of *C. albicans*[5] and hyphal formation is associated with important virulence traits such as toxin and protease production, adhesion, invasion, and immune system activation[17]. Thus, we first asked whether neutrophil recruitment was impaired during infection with the *hgc1Δ/Δ C. albicans* strain which cannot filament *in vivo*[18]. Indeed, infection with hypha-deficient *hgc1Δ/Δ C. albicans* significantly impaired neutrophil recruitment and enhanced fungal CNS tissue invasion relative to the isogenic wild-type *C. albicans* strain (Fig. 4a). Thus, strikingly, filamentation is not required for *C. albicans* invasion of brain tissue, in contrast to other organs such as the kidney[18].

Candidalysin is a recently-described peptide toxin encoded by *ECE1* and expressed exclusively by *C. albicans* hyphae[19]. Candidalysin was shown to mediate epithelial cell damage via pore formation in the plasma cell membrane resulting in IL-1α release and pro-inflammatory cytokine production. Hence, Candidalysin-null mutants were highly attenuated in murine oropharyngeal and vulvovaginal candidiasis models[19-21]. Instead, we found that lack of Candidalysin promoted brain infection, and that this phenotype was specific to the Candidalysin peptide since mutant strains deficient in the entire gene (*ece1Δ/Δ*) or specifically in the Candidalysin-encoding portion of the gene (*ece1Δ/Δ + ECE1$_{Δ184-279}$*) were both hyper-virulent for *C. albicans* brain invasion (Fig. 4b).

The increased ability of the Candidalysin-null mutants to proliferate within the brain directly correlated with the degree of neutrophil recruitment. We found a near absence of neutrophils in the brains of wild-type animals infected with Candidalysin-null strains and observed hyphal forms growing in the brain parenchyma without neutrophilic reaction (Fig. 4c). In contrast, the Candidalysin-producing parental strain and the re-integrant control strain promoted neutrophil recruitment at 24 h post-infection, and these neutrophils clustered around invading hyphae (Fig. 4c). In line with the absence of neutrophils in the brains of mice infected with Candidalysin-null strains, IL-1β and CXCL1 were significantly reduced in brain homogenates from animals infected with these strains (Fig. 4d). Therefore, Candidalysin is a key fungal factor that activates the IL-1β–CXCL1 protective pathway *in vivo*. Notably, in contrast to its role in the mucosa, Candidalysin acts as an avirulence factor in the brain by instigating protective host CNS immunity, underscoring the tissue-specific opposing roles that a microbial factor may play during infection with the same pathogen[17].

We next wondered whether other *C. albicans* hyphae-associated secreted proteins also activate protective neutrophil responses in the brain. Secreted aspartyl proteases (Saps) are enzymes with extracellular proteolytic activity and are linked to virulence[22]. *C. albicans* Saps promote neutrophil recruitment during vulvovaginal candidiasis in mice[23,24]. Expression of the *SAP4-6* subfamily is coordinately regulated with hyphal formation[22], therefore we tested whether these hyphal-associated Saps contributed towards virulence during brain invasion. Wild-type animals infected with the triple-deficient strain *sap4/5/6Δ/Δ* had comparable brain fungal burdens to animals infected with the complemented control strain (Fig. 4e). In line with this, we saw no difference in CNS neutrophil recruitment in

these animals, indicating that *C. albicans* Saps exhibit tissue-specific roles in promoting neutrophil recruitment during infection[23,24] (Fig. 4e). Therefore, protective CNS neutrophil recruitment is activated by Candidalysin, and not by other *C. albicans* hyphae-secreted enzymes.

Candidalysin Drives Microglial IL-1β and CXCL1 *in vivo*

We next sought to define the Candidalysin-responsive CNS immune cells post-infection. We infected wild-type mice with the parental strain of *C. albicans* (BWP17) or the Candidalysin-null strain (*ece1Δ/Δ*), and analyzed IL-1β and CXCL1 production at 24 h post-infection. Although all brain phagocytes produced both IL-1β and CXCL1, microglia were the only population to exhibit dependence on Candidalysin, since microglia isolated from *ece1Δ/Δ*-infected brains produced significantly less IL-1β and CXCL1 *ex vivo* (Fig. 5a,b). Instead, Ly6C^{hi} monocytes and neutrophils did not depend on Candidalysin for IL-1β and CXCL1 production, suggesting that other as-yet unidentified fungal factors activate this pathway in these phagocytes. Together, our data show that Candidalysin acts on microglia to stimulate IL-1β release, which then drives CXCL1 production that is required for protective neutrophil CNS recruitment.

Candidalysin Drives Differing Glial IL-1β–CXCL1 *ex vivo*

To gain mechanistic insights into how microglia respond to Candidalysin, we cultured the microglia cell line BV-2[25] in the presence of synthetic Candidalysin and measured IL-1β and CXCL1 in the supernatants. In line with our *in vivo* work, we found time- and dose-dependent IL-1β production by BV-2 cells in response to Candidalysin (Fig. 6a). However, we did not detect CXCL1 from BV-2 cells stimulated under these conditions. We first considered that this could be due to Candidalysin-induced damage that may prevent BV-2 cells from producing CXCL1 after IL-1β secretion. Indeed, as shown for epithelial cells[19], Candidalysin mediated dose-dependent cell damage to BV-2 microglia (Fig. 6b). Alternatively, additional signals beyond IL-1β, derived from non-microglial CNS cells, might be required for microglial CXCL1 induction, acting *in trans*. To test this hypothesis, we co-cultured BV-2 cells with immortalized C8-D1A astrocytes in the presence of Candidalysin and measured IL-1β and CXCL1 in the supernatants. We chose astrocytes since they are known to respond to IL-1β to produce inflammatory mediators, including CXCL1, in other models of CNS inflammation[26-28]. We found that astrocytes responded to Candidalysin to produce CXCL1 (Fig. 6c), but not IL-1β (data not shown), and that CXCL1 production significantly increased when astrocytes and microglia were co-cultured (Fig. 6c). To confirm that microglia are a relevant cellular source of CXCL1 detected during microglia-astrocyte co-culture, we performed intracellular staining for CXCL1 and found that BV-2 microglia are significant producers of CXCL1 in response to Candidalysin, but only when astrocytes were present (Fig. 6d). Therefore, astrocytes provide additional signals to microglia that are needed for CXCL1 production in response to Candidalysin.

We next investigated the pathway activated by Candidalysin in BV-2 microglia to produce IL-1β. Candidalysin was previously shown in epithelial cells to activate c-Fos, in a p38-dependent manner, and the phosphatase MKP-1[20]. We thus asked whether the same pathways are activated by Candidalysin in BV-2 microglia. We found that Candidalysin

sequentially and dose-dependently activated MKP-1 and c-Fos (Fig. 6e), and chemical inhibition of p38 or c-Fos significantly reduced IL-1β release by Candidalysin-stimulated BV-2 cells (Fig. 6f). Therefore, microglia produce IL-1β in response to Candidalysin via activation of p38 and c-Fos.

The Microglial IL-1β–CXCL1 Response Requires CARD9

CARD9-deficiency is the only known risk factor that uniquely predisposes to CNS candidiasis in the absence of iatrogenic intervention[2,5]. We first examined whether CARD9-deficiency causes developmental defects in resident microglia, but found no defects in abundance or activation markers at steady state in *Card9*^{−/−} microglia, which accumulated in similar numbers as wild-type microglia after fungal infection (Supplementary Fig. 5). Since *C. albicans* activates the microglial IL-1β–CXCL1 axis to regulate protective neutrophil CNS recruitment, we next analyzed the dependence on CARD9 for induction of this pathway in microglia post-infection *in vivo*. We hypothesized that CARD9 is required for these functions, as microglia highly-express CARD9 and we previously found reduced transcription of CXC chemokines by *Card9*^{−/−} microglia harvested from the *C. albicans*-infected brain[5]. We infected *Card9*^{+/+} and *Card9*^{−/−} animals with wild-type Candidalysin-expressing *C. albicans*, isolated phagocytes from the brain and measured pro-IL-1β and CXCL1 production following *ex vivo* restimulation. We found significantly decreased frequencies of CXCL1^{+} and pro-IL-1β^{+} cells in the fungal-infected *Card9*^{−/−} brain, and these decreases mapped to microglia (Fig. 7a,b).

Since production and secretion of mature IL-1β depends on pro-IL-1β expression and consecutive inflammasome-dependent processing, we asked whether microglia depend on CARD9 for pro-IL-1β transcription and/or inflammasome activation. We FACS-sorted microglia from wild-type and *Card9*^{−/−} infected brains, and examined *Il1b* transcription by qRT-PCR, and levels of pro-IL-1β and cleaved and pro-caspase-1 by immunoblot. We found significantly decreased *Il1b* transcription in *Card9*^{−/−} microglia, which we confirmed at the protein level (Fig. 7c,d). These data are in line with the reported CARD9-dependent pro-IL-1β transcription in bone marrow-derived dendritic cells post-viral infection[29]. We also found significantly reduced cleaved caspase-1 in *Card9*^{−/−} microglia (Fig. 7d), indicating that Card9 also operates at the level of inflammasome activation for IL-1β production. Given that c-Fos mediated Candidalysin-induced IL-1β production by BV-2 cells, we measured c-Fos expression in WT and *Card9*^{−/−} microglia by immunoblot and found significantly decreased c-Fos expression in *Card9*^{−/−} microglia (Fig. 7d).

We next examined the NLRP3 inflammasome in FACS-sorted WT and *Card9*^{−/−} microglia. We focused on NLRP3 because CARD9 was reported to negatively regulate NLRP3 activation during macrophage *Salmonella* infection[30], and we recently showed that Candidalysin activates NLRP3 in bone marrow-derived macrophages[31]. We found significantly decreased NLRP3 protein expression in *Card9*^{−/−} microglia (Fig. 7e). Of interest, *Nlrp3*^{−/−} animals had significantly decreased neutrophil accumulation to the *C. albicans*-infected brain and increased fungal load post-infection, consistent with a potential role of Card9-dependent NLRP3-inflammasome activation for protective neutrophil influx in the fungal-infected CNS (Fig. 7f). Together, microglia require CARD9 for c-Fos activation

and for production of mature IL-1β via *Il1b* transcriptional regulation and inflammasome activation, to activate the IL-1β–CXCL1 axis in response to fungal invasion.

Microglial CARD9 Deletion Causes CNS Fungal Invasion

We next directly examined the impact of genetic *Card9* deletion specifically within microglia by utilizing mice expressing tamoxifen-inducible Cre recombinase under the *Cx3cr1* promoter (*Cx3cr1*[CreER])[32]. These mice has been used to genetically manipulate long-lived CX3CR1[+] microglia while leaving short-lived CX3CR1[+] monocytes and monocyte-derived macrophages unaffected. We bred *Cx3cr1*[CreER] animals to Card9-floxed mice[11], tamoxifen-pulsed the progeny to activate Cre expression and waited 4-6 weeks to allow replenishment of short-lived non-microglia CX3CR1^{+} cells from the bone marrow, while long-lived microglia remained Card9-deficient (Supplementary Fig. S6). *C. albicans* infection of *Card9*^{fl/fl}*Cx3cr1*[CreER+/−] animals revealed a significant dependence on *Card9* expression by the long-lived CX3CR1[+] cellular compartment for control of fungal brain growth (Fig. 8a), while renal fungal control was unaffected in microglia-specific conditional *Card9*^{−/−} mice (Fig. 8a).

To analyze whether the susceptibility to brain infection in *Card9*^{fl/fl}*Cx3cr1*[CreER+/−] mice was related to a neutrophil recruitment defect, we quantified neutrophils within the infected brains of *Card9*^{fl/fl}*Cx3cr1*[CreER+/−] mice and their Cre-negative littermates. We found that microglial deletion of *Card9* significantly reduced the protective early influx of neutrophils into the fungal-infected brain (Fig. 8b), which correlated with significantly decreased expression of microglial pro-IL1β and CXCL1 in the conditional *Card9*^{−/−} mice (Fig. 8c). Together, our data shows that CARD9-expressing microglia orchestrate control of fungal brain invasion by responding to fungus-secreted Candidalysin to produce IL-1β–induced CXCL1, which recruits CXCR2-expressing neutrophils that mediate CNS fungal clearance (Supplementary Fig. S7).

Discussion

Herein, we demonstrate the critical contribution of CARD9-mediated IL-1β and CXCL1 in recruiting protective neutrophils to the fungal-infected CNS. We identify microglia as major producers of CARD9-dependent IL-1β and CXCL1 during *C. albicans* CNS invasion and the fungal-secreted toxin Candidalysin as a critical pathogen-derived factor activating this pathway. Our study offers novel insights into the network of host and fungal factors that protect against CNS fungal invasion and unveil the mechanism of CNS fungal susceptibility in inherited CARD9-deficiency.

Systemic candidiasis is a leading cause of nosocomial bloodstream infection with mortality >50% despite therapy[33]. Neutropenia is the major predisposing factor for systemic candidiasis and *Candida* CNS invasion in particular[1,34]. Moreover, CNS invasion is prevalent during systemic candidiasis in low-birth weight neonates and also occurs as an iatrogenic complication post-neurosurgical procedures[35,36]. Strikingly, CARD9-deficiency is a primary immunodeficiency disorder (PID) characterized by heightened susceptibility to fungal infections of which CNS candidiasis is a hallmark[2,34]. CARD9-deficiency is the only known PID that causes fungal-specific infection susceptibility without other infectious or

non-infectious manifestations, and the only PID that causes fungal disease in which CNS is a primary target tissue[17]. We previously demonstrated that *Candida* CNS disease in CARD9-deficiency is caused by a fungal- and brain-specific defect in neutrophil recruitment[5]. CNS neutropenia is now confirmed in several CARD9-deficient patients with CNS candidiasis[7,37,38]. Nonetheless, how CARD9 mediates protective neutrophil trafficking into the fungal-infected CNS remained unclear.

Our analysis of mice deficient in several CLR, cytokine and chemokine circuits uncovered 1) the functional redundancy among CLRs, which may suggest the presence of yet-undiscovered CARD9-coupled receptors for driving tissue-specific antifungal defense; 2) the indispensable role of the CARD9-partner MALT1 in controlling CNS fungal invasion independent of neutrophil recruitment, which implies that $MALT1^{-/-}$ patients may be at risk for CNS fungal disease; and 3) the critical contribution of IL-1β–CXCL1-mediated neutrophil recruitment for control of CNS fungal invasion. CXCR2 was known to mediate neutrophil trafficking during viral infection, parasitic meningitis[39] and fungal pneumonia[40], and herein we reveal its importance for recruiting neutrophils during fungal CNS infection, principally through binding CXCL1. In contrast, CCR1, CXCR1 and LTB4R1 are dispensable despite them regulating neutrophil recruitment and function in other *C. albicans*-infected tissues[13-15]. These studies further underscore the organ- and context-specific dependence on chemotactic molecules for protective host immunity.

We showed that IL-1β is required for CXCL1 induction, in line with earlier work which showed IL-1β–induced CXCL1 production controlling neutrophil accumulation during bacterial peritonitis and autoimmune, traumatic or bacterial neuroinflammation[10,41,42]. Importantly, microglia are the primary myeloid cellular source of IL-1β-dependent CXCL1 production *in vivo*. During oral candidiasis, IL-1R is also required for neutrophil accumulation to the oral mucosa[8], as we showed for systemic infection in the brain. However, further attesting to the presence of tissue-specific anti-*Candida* immune response cues, the IL-1R–dependent response in the oral epithelium is largely controlled by IL-1α released by damaged keratinocytes[8], whereas we found that IL-1α plays a modest role in controlling brain fungal invasion. In fact, IL-1α release by both oral and vaginal epithelial cells is driven by exposure to the fungal-secreted toxin Candidalysin[19-21].

Candidalysin enables the establishment of *C. albicans* mucosal infections, since Candidalysin-deficient strains are avirulent in these models[19,21]. In contrast, we found that Candidalysin-deficient strains are hyper-virulent for the brain, associated with decreased IL-1β and CXCL1 production and impaired neutrophil recruitment. These results indicate that Candidalysin is not only a classical virulence factor, but also an immune modulator, which exerts context-specific effects on the immune system. We propose that this dual function of Candidalysin is the result of a co-evolutionary event; the fungus developed an efficient toxin to damage host membranes, and, in response, the host evolved a sensitive Candidalysin detection system to defend against this common mucosal pathogen. Whether Candidalysin is recognized by a specific microglial innate receptor to mediate the protective IL-1β–CXCL1 axis is unclear, since the toxin mediates cellular damage which could also activate glial cells. Therefore, identifying how host epithelial and immune cells recognize Candidalysin merits investigation.

We found that Candidalysin selectively activates microglia for IL-1β and CXCL1 production, a self-renewing macrophage population that contributes towards neuroinflammation in neurodegenerative disorders and promotes pathogen and dead cell clearance within the CNS[43]. Interestingly, downstream of Candidalysin-induced microglial IL-1β secretion, which occurs via c-Fos activation, we show that additional signals derived from astrocytes acting *in trans* are required for microglia to secrete CXCL1. Whether direct microglia-astrocyte contact is required or astrocyte-derived soluble factors acting on microglia are needed remains unknown. Indeed, microglia are known to interact with astrocytes to drive or suppress inflammation[44,45]. Therefore, the molecular factors that drive microglia-astrocyte cross-talk within the fungal-infected brain warrant further investigation.

Lastly, we examined the dependence on CARD9 for the microglia-mediated, IL-1β −CXCL1-dependent pathway that recruits protective neutrophils, using fully Card9-deficient and conditional microglia-specific *Card9^−/−* mice. We show that CARD9 is critical for c-Fos activation and for the production of both IL-1β and CXCL1 by microglia in the infected CNS operating at the levels of both transcriptional pro-IL-1β regulation and inflammasome activation for IL-1β generation, with NLRP3 being at least partly involved, as shown with *Microsporum* infection[46]. Together, these data shed light into the pathogenesis of inherited CARD9-deficiency by outlining a pathway of CARD9-dependent microglial production of sequential IL-1β and CXCL1 that recruits protective neutrophils into the fungal-infected CNS.

Future studies should examine whether Card9 promotes microglial innate functions beyond orchestrating neutrophil recruitment such as fungal uptake and killing. Of note, the phenotype of microglia-specific conditional knockout mice is less severe than that of *Card9^−/−* mice, which may reflect the important role of astrocytes, which express Card9 post-infection[5], in priming microglial CXCL1 production. Future work should examine whether non-CNS tissue-resident macrophages, such as Kupffer cells differentially depend on Card9 for IL-1β−CXCL1-mediated neutrophil recruitment, as previously shown for differential macrophage and dendritic cell-induced Card9-dependent TNF-α[47]; this will help further understand the fungal infection CNS-specificity in CARD9-deficiency. Beyond understanding the pathogenesis of inherited CARD9-deficiency, our findings have important implications for recognizing the potential fungal infection risk in patients who are increasingly receiving Syk inhibitors for autoimmune and malignant diseases[48,49]. Surveillance of Syk inhibitor-treated patients and research in conditional Syk-deficient mice will help determine their CNS fungal disease risk.

In summary, we present evidence of an intricate host immune pathway that protects the CNS from invading fungi. This work uncovers the complex interactions occurring between the host and the most common human fungal pathogen within the CNS, and sheds novel mechanistic light into the pathogenesis of inherited CARD9-deficiency.

Methods

Mice

Animals (males and females) were used at 8-12 weeks of age and were maintained in individually ventilated cages under specific pathogen-free conditions at the 14BS facility at the National Institutes of Health (Bethesda, MD, USA), the Memorial Sloan Kettering Cancer Center Comparative Medicine Shared Resources (New York, NY, USA), or the Medical Research Facility at the University of Aberdeen (UK). The following strains (and their respective WT controls/littermates) were obtained from the NIAID Taconic contract; $Cxcr2^{-/-}$, $Il1r^{-/-}$, $Ltb4r1^{-/-}$, $Fpr1^{-/-}$. All other strains and their respective controls/littermates were bred in-house at the NIH ($Clec7a^{-/-}$, $Clec4n^{-/-}$, $Clec4e^{-/-}$, $Myd88^{-/-}$, $Ccr1^{-/-}$, $Cxcr1^{-/-}$, $Cxcl1^{-/-}$, $Il1a^{-/-}$, $Il1b^{-/-}$, $Il1a^{-/-}Il1b^{-/-}$, $Nlrp3^{-/-}$, $Card9^{fl/fl}Cx3CR1^{CreER+/-}$), Memorial Sloan-Kettering Cancer Center ($Clec7a^{-/-}Fcer1g^{-/-}$), University of Aberdeen ($Clec4d^{-/-}$), or USUHS ($Malt1^{-/-}$)[51]. Mice homozygous for the $Card9^{tm1a}$ allele were purchased from the Wellcome Trust Sanger Institute (EUCOMM Project No. 44813), and these animals were bred with the FLPer deleter strain (Jackson Laboratories) to remove the FRT-flanked knock-out first cassette, generating $Card9^{tm1c}$ homozygous mice (referred to as $Card9^{fl/fl}$ in this manuscript)[52,53]. Homozygous $Card9^{fl/fl}$ animals were bred with heterozygous $Cx3cr1^{CreER}$ transgenic animals (Jackson Laboratories) to generate $Card9^{fl/fl}Cx3cr1^{CreER+/-}$ mice and littermate controls. Soon after weaning (~5-6 weeks old), $Card9^{fl/fl}Cx3cr1^{CreER+/-}$ mice and their controls were treated with two 10mg doses of tamoxifen (Sigma) administered in corn oil by oral gavage, given 48 h apart. After 4-6 weeks, these animals were infected and analyzed as outlined in the Figure legends. All experimentation conformed to conditions approved by the Animal Care and Use Committee of the National Institute of Allergy and Infectious Diseases.

Candidiasis Model and Fungal Burden Determination

Candida albicans strains used in this study were SC5314, BWP17, $ece1\Delta/\Delta$, $ece1\Delta/\Delta+ECE1$, $ece1\Delta/\Delta+ECE1_{\Delta184-279}$ [19], CAI4+CIp10 and $sap4/5/6\Delta/\Delta$, and $hgc1\Delta/\Delta$ and $hgc1\Delta/\Delta + HGC1$[18]. Yeast was serially passaged three times in YPD broth, grown at 30°C with shaking for 18-24 h at each passage. Yeast cells were washed in PBS, counted, and injected intravenously via the lateral tail vein. Animals were infected with 1.3×10^5 colony forming units (CFU) for analysis at 24 h post-infection, or 7×10^4 CFU for analysis at 72 h post-infection, unless otherwise stated in the corresponding Figure legends. For analysis of brain fungal burdens, animals were euthanized and brains weighed, homogenized in PBS, and serially diluted before plating onto YPD agar supplemented with Penicillin/Streptomycin (Invitrogen). Colonies were counted after incubation at 37°C for 24-48 h.

Analysis of Brain Neutrophil Recruitment by FACS

Leukocytes were isolated from brains using previously described methods[54], resuspended in PBS and stained with Live/Dead fluorescent dye (Invitrogen) for 10 min on ice. Cells were then stained with fluorophore-conjugated antibodies in the presence of anti-CD16/32 and 0.5% BSA for 30 min on ice. Samples were washed in PBS/0.5% BSA/0.01% sodium azide and acquired using the BD Fortessa instrument equipped with BD FACS Diva software (BD Biosciences). FlowJo (TreeStar) was used for the final analysis. Anti-mouse antibodies used

in this study were: CD45 (30-F11), CD11b (M1/70), both from eBiosciences, and Ly6G (1A8), Ly6C (AL-21), both from BD Biosciences.

Histology

Brains were removed from infected mice at the indicated time points and fixed in 10% formalin for 24 h before embedding in paraffin wax. Tissue sections were stained with periodic acid-Schiff (PAS).

Measurement of Cytokines and Chemokines in Brain Homogenates

Infected brains were isolated at 24 h post-infection and homogenized in 1 mL PBS supplemented with 0.05% Tween20 and protease inhibitor cocktail (Roche). Homogenized brains were centrifuged twice to remove debris and resulting supernatants snap-frozen on dry ice and stored at −80 °C prior to analysis. IL-1β and CXCL1 concentrations in the homogenates was determined by ELISA (R&D Systems), following the manufacturers' instructions.

Ex Vivo Restimulations and Intracellular FACS Analysis

Animals were infected with 2×10^5 CFU of the indicated *C. albicans* strains intravenously, and brain leukocytes isolated 24 h later. For these experiments, brains were first digested in RPMI supplemented with 0.8 mg/mL Dispase (Gibco), 0.2mg/mL Collagenase Type 4 (Worthington), and 0.1 mg/mL DNAse (Roche) at 37 °C for 30 min, then pipetted vigorously to create a homogenous suspension. These suspensions were centrifuged (1500 rpm, 5 min, 4 °C), pellets resuspended in 5 mL 40% Percoll (GE Healthcare) and centrifuged again at 1700 rpm for 20 min at 4 °C to remove myelin. Cell pellets were washed in RPMI supplemented with 10% heat-inactivated fetal bovine serum and Penicillin/Streptomycin (Invitrogen), and added to FACS tubes for stimulations. Cells were incubated for 4 h at 37 °C in the presence of 5 μg/mL Brefeldin A (Sigma) and, where indicated, 1 μg/mL LPS (Sigma) or 62.5 μg/mL depleted zymosan (Sigma). After stimulation, cells were washed in PBS and stained for surface markers as above. Fixation/permeabilization was performed with the eBioscience Foxp3 staining kit, and staining for CXCL1 (IC4532R, from R&D Systems) or pro-IL-1β (NJTEN3; from eBioscience) performed overnight at 4 °C. Samples were washed once in PBS/0.5% BSA/0.01% sodium azide prior to acquisition using the BD Fortessa instrument equipped with BD FACS Diva software (BD Biosciences). FlowJo (TreeStar) was used for the final analysis. CXCL1$^+$ and pro-IL-1β$^+$ cells were determined by employing similar staining and gating in animals deficient in these mediators (*Cxcl1*$^{−/−}$, *Il1b*$^{−/−}$) as negative controls.

Cell Culture and Candidalysin Stimulations

BV-2 cells were kindly provided by F. Crews (University of North Carolina School of Medicine). C8-D1A astrocytes were kindly provided by D. McGavern (NINDS, NIH). Details regarding the validation and use of these cell lines are provided in the Life Sciences Reporting Summary. BV-2 were maintained at 37 °C, 5% CO_2 in RPMI supplemented with L-glutamine and HEPES (pH 7.0 – 7.4; Corning), 10% heat-inactivated fetal bovine serum and Penicillin/Streptomycin (Invitrogen). DMEM media was used as the base media for C8-

D1A culture, with the same supplements as listed above and cultured as for BV-2. For BV-2 single culture experiments, cells were lifted using cell scrapers and seeded into 24 well-plates at 5×10^5 cells/well (BV-2) and left to adhere for 2 h at 37°C with either: 50 ng/mL LPS (Sigma), T-5224 (APExBIO) and/or SB203580 (Adipogen); see Figure legends for details of each experiment. After 2 h, recombinant Candidalysin peptide (Peptide Protein Research) was added to the cells at the indicated concentrations and incubation at 37 °C continued. For co-culture experiments, 3×10^5 C8-D1A were added to each well of a 24 well-plate and incubated overnight at 37 °C. BV-2 cells and Candidalysin were added as described above. In both types of experiments, supernatants or cells were collected at the indicated time points after Candidalysin addition and analyzed for IL-1β and CXCL1 by ELISA (R&D Systems), CXCL1 staining by intracellular flow cytometry, or by immunoblot.

Immunoblot Analysis

Whole cell lysates were suspended in RIPA buffer containing protease and phosphatase inhibitors (Thermo Scientific). Lysates were separated in SDS-PAGE and transferred to a nitrocellulose membrane, 0.2 μm (Bio-Rad Laboratories). The membrane was incubated with the following primary antibodies: phospho-MPK1/MPK2 polyclonal [Ser296, Ser318] (Thermo Scientific) and c-Fos (Cell Signaling), IL-1β [3A6] (Cell Signaling), Caspase-1 p20 [Casper-1] (Adipogen Life Sciences) (Thermo Scientific), NLRP3 [D4D8T] (Cell Signaling). Normalization was performed by probing the membrane with β-Actin antibody (Cell Signaling). Chemiluminescence detection was performed with Clarity™ Western ECL Substrate (Bio-Rad Laboratories), using the ChemiDoc™ MP Imaging System (Bio-Rad).

FACS/MACS Sorting of Microglia

Wild-type animals were infected with 1.3×10^5 CFU SC5314 and euthanized at 24 h post-infection. Brains were digested as above and leukocytes stained with sterile antibodies[55]. Ly6C^{hi} monocytes (CD45^{hi} CD11b^{+} Ly6C^{hi} Ly6G^{−}) and microglia (CD45^{lo} CD11b^{+} Ly6G^{−} Ly6C^{−}) were FACS-sorted into sterile sorting buffer (HBSS supplemented with 2 mM EDTA, 10 % FCS, 100 U/mL penicillin, 100 μg/mL streptomycin) using a FACS Aria instrument for downstream qRT-PCR and immunoblot analyses. Purity of cells were greater than >95%, on average. In some experiments (qRT-PCR of CLRs in brain-resident microglia; Supplementary Fig. 1), microglia were instead sorted by magnetic separation using anti-CD11b microbeads (Miltenyi). Cells were then centrifuged (1500 rpm 5 min, 4 °C) and resuspended in Trizol for RNA purification or RIPA buffer for downstream immunoblot analysis. Depending on the experiment, up to 5 animals were pooled for individual sorts, or individual mice were analyzed separately (see Figure legends for details).

Generation of cDNA and qRT-PCR

RNA was extracted from sorted brain myeloid cells (defined using the gating strategy shown in Supplementary Fig. 2) using Trizol (Invitrogen) and the RNeasy kit (Qiagen) per the manufacturer's protocol. Purified RNA was used as a template for cDNA generation using the qScript cDNA SuperMix kit (Quanta Biosciences) with oligodT and random primers. Quantitative PCR was performed by TaqMan detection (PerfeCTa qPCR FastMix ROX; Quanta BioSciences) with the 7900HT Fast Real-Time PCR System (Applied Biosystems). All qPCR assays were performed in duplicate and the relative gene expression of each gene

was determined after normalization with GAPDH transcript levels using the ΔΔCT method. TaqMan primers/probes (*Clec7a, Clec4n, Clec4d, Clec4e, Il1b, Card9, Gapdh*) were predesigned by Applied Biosystems.

Statistics

Statistical analyses were performed using GraphPad Prism 7.0 software. Details of individual tests are included in the figure legends. In general, data was tested for normal distribution by Kolmogorov-Smirnov normality test and analyzed accordingly by two-tailed unpaired t-tests or two-tailed Mann Whitney U-test. In cases where multiple data sets were analyzed, two-way ANOVA was used with Bonferroni correction. In all cases, *P* values <0.05 were considered significant. Further details relating to power calculations, randomization and blinding are described in the Life Sciences Reporting Summary.

Data Availability

The data that support the findings of this study are available from the corresponding authors upon request.

Supplementary Material

Refer to Web version on PubMed Central for supplementary material.

Acknowledgements

References

1. Lionakis MS & Levitz SM Host control of fungal infections: lessons from basic studies and human cohorts. Ann Rev Immunol 36, 157–191 (2018). [PubMed: 29237128]

2. Drummond RA & Lionakis MS Mechanistic insights into the role of C-type lectin receptor/CARD9 signaling in human antifungal immunity. Front Cell Infect Microbiol 6, 10.3389/fcimb.2016.00039 (2016).

3. Glocker EO, Hennigs A, Nabavi M, Schaffer AA, Woellner C et al. A homozygous CARD9 mutation in a family with susceptibility to fungal infections. N Engl J Med 361, 1727–1735 (2009). [PubMed: 19864672]

4. Lanternier F, Pathan S, Vincent QB, Liu L, Cypowyj S et al. Deep dermatophytosis and inherited CARD9 deficiency. N Engl J Med 369, 1704–1714 (2013). [PubMed: 24131138]

5. Drummond RA, Collar AL, Swamydas M, Rodriguez CA, Lim JK et al. CARD9-dependent neutrophil recruitment protects against fungal invasion of the central nervous system. PLoS Pathog 11, e1005293 (2015). [PubMed: 26679537]

6. Li X, Utomo A, Cullere X, Choi MM, Milner DA Jr. et al. The β-glucan receptor Dectin-1 activates the integrin Mac-1 in neutrophils via Vav protein signaling to promote Candida albicans clearance. Cell Host Microbe 10, 603–615 (2011). [PubMed: 22177564]

7. Drewniak A, Gazendam RP, Tool ATJ, van Houdt M, Jansen MH et al. Invasive fungal infection and impaired neutrophil killing in human CARD9 deficiency. Blood 121, 2385–2392 (2013). [PubMed: 23335372]

8. Altmeier S, Toska A, Sparber F, Teijeira A, Halin C et al. IL-1 coordinates the neutrophil response to C. albicans in the oral mucosa. PLOS Pathog 12, e1005882 (2016). [PubMed: 27632536]

9. Karki R, Man SM, Malireddi RKS, Gurung P, Vogel P et al. Concerted activation of the AIM2 and NLRP3 inflammasomes orchestrates host protection against Aspergillus infection. Cell Host Microbe 17, 357–368 (2015). [PubMed: 25704009]

10. Biondo C, Mancuso G, Midiri A, Signorino G, Domina M et al. The interleukin-1β/CXCL½/ neutrophil axis mediates host protection against group B Streptococcal infection. Infect Immun 82, 4508–4517 (2014). [PubMed: 25114117]

11. Nemeth T, Futosi K, Sitaru C, Ruland J & Mocsai A Neutrophil-specific deletion of the CARD9 gene expression regulator suppresses autoantibody-induced inflammation in vivo. Nat Commun 7, 11004 (2016). [PubMed: 27032818]

12. Wang X, Zhang R, Wu W, Song Y, Wan Z et al. Impaired specific antifungal immunity in CARD9-deficient patients with phaeohyphomycosis. J Investig Dermatol 138, 607–617 (2018). [PubMed: 29080677]

13. Lionakis MS, Fischer BG, Lim JK, Swamydas M, Wan W et al. Chemokine receptor Ccr1 drives neutrophil-mediated kidney immunopathology and mortality in invasive candidiasis. PLoS Pathog 8, e1002865 (2012). [PubMed: 22916017]

14. Lee EKS, Gillrie MR, Li L, Arnason JW, Kim JH et al. Leukotriene B4-mediated neutrophil recruitment causes pulmonary capillaritis during lethal fungal sepsis. Cell Host Microbe 23, 121–133.e124 (2018). [PubMed: 29290576]

15. Swamydas M, Gao J-L, Break TJ, Johnson MD, Jaeger M et al. CXCR1-mediated neutrophil degranulation and fungal killing promote Candida clearance and host survival. Sci Trans Med 8, 322ra310–322ra310 (2016).

16. Ngo LY, Kasahara S, Kumasaka DK, Knoblaugh SE, Jhingran A et al. Inflammatory monocytes mediate early and organ-specific innate defense during systemic candidiasis. J Infect Dis 209, 109–119 (2014). [PubMed: 23922372]

17. Erwig LP & Gow NAR Interactions of fungal pathogens with phagocytes. Nat Rev Microbiol 14, 163–176 (2016). [PubMed: 26853116]

18. Zheng X, Wang Y & Wang Y Hgc1, a novel hypha-specific G1 cyclin-related protein regulates Candida albicans hyphal morphogenesis. EMBO J 23, 1845–1856 (2004). [PubMed: 15071502]

19. Moyes DL, Wilson D, Richardson JP, Mogavero S, Tang SX et al. Candidalysin is a fungal peptide toxin critical for mucosal infection. Nature 532, 64–68 (2016). [PubMed: 27027296]

20. Verma AH, Richardson JP, Zhou C, Coleman BM, Moyes DL et al. Oral epithelial cells orchestrate innate type 17 responses to Candida albicans through the virulence factor candidalysin. Sci Immunol 2 10/1126/sciimmunol.aam8834 (2017).

21. Richardson JP, Willems HME, Moyes DL, Shoaie S, Barker KS et al. Candidalysin drives epithelial signaling, neutrophil recruitment, and immunopathology at the vaginal mucosa. Infect Immun, 10.1128/IAI.00645-00617 (2017).

22. Naglik JR, Challacombe SJ & Hube B Candida albicans secreted aspartyl proteinases in virulence and pathogenesis. Microbiol Mol Biol Rev 67, 400–428 (2003). [PubMed: 12966142]

23. Gabrielli E, Sabbatini S, Roselletti E, Kasper L, Perito S et al. In vivo induction of neutrophil chemotaxis by secretory aspartyl proteinases of Candida albicans. Virulence 7, 819–825 (2016). [PubMed: 27127904]

24. Pericolini E, Gabrielli E, Amacker M, Kasper L, Roselletti E et al. Secretory aspartyl proteinases cause vaginitis and can mediate vaginitis caused by Candida albicans in mice. mBio 6, e00724–00715 (2015). [PubMed: 26037125]

25. Henn A, Lund S, Hedtjarn M, Schrattenholz A, Porzgen P et al. The suitability of BV2 cells as alternative model system for primary microglia cultures or for animal experiments examining brain inflammation. Altex-Alternativen Zu Tierexperimenten 26, 83–94 (2009).

26. Hennessy E, Griffin ÉW & Cunningham C Astrocytes are primed by chronic neurodegeneration to produce exaggerated chemokine and cell infiltration responses to acute stimulation with the cytokines IL-1β and TNF-α. J Neurosci 35, 8411–8422 (2015). [PubMed: 26041910]

27. Pineau I, Sun L, Bastien D & Lacroix S Astrocytes initiate inflammation in the injured mouse spinal cord by promoting the entry of neutrophils and inflammatory monocytes in an IL-1 receptor/MyD88-dependent fashion. Brain Behav Immun 24, 540–553 (2010). [PubMed: 19932745]

28. Omari KM, John G, Lango R & Raine CS Role for CXCR2 and CXCL1 on glia in multiple sclerosis. Glia 53, 24–31 (2005).

29. Poeck H, Bscheider M, Gross O, Finger K, Roth S et al. Recognition of RNA virus by RIG-I results in activation of CARD9 and inflammasome signaling for interleukin 1β production. Nature Immunol 11, 63–69 (2009). [PubMed: 19915568]

30. Pereira M, Tourlomousis P, Wright J, P Monie T & Bryant CE CARD9 negatively regulates NLRP3-induced IL-1β production on Salmonella infection of macrophages. Nature Commun 7, 12874–12874 (2016). [PubMed: 27670879]

31. Kasper L, König A, Koenig P-A, Gresnigt MS, Westman J et al. The fungal peptide toxin Candidalysin activates the NLRP3 inflammasome and causes cytolysis in mononuclear phagocytes. Nature Commun 9, 4260 (2018). [PubMed: 30323213]

32. Parkhurst CN, Yang G, Ninan I, Savas JN, Yates JR et al. Microglia promote learning-dependent synapse formation through BDNF. Cell 155, 1596–1609 (2013). [PubMed: 24360280]

33. Pappas PG, Lionakis MS, Arendrup MC, Ostrosky-Zeichner L & Kullberg BJ Invasive candidiasis. Nat Rev Dis Primers 4, 18026 (2018). [PubMed: 29749387]

34. Lionakis MS, Netea MG & Holland SM Mendelian genetics of human susceptibility to fungal infection. Cold Spring Harbor Perspect Med 4 10.1101/cshperspect.a019638 (2014).

35. McCarthy MW, Kalasauskas D, Petraitis V, Petraitiene R & Walsh TJ Fungal infections of the central nervous system in children. J Pediatric Infect Dis Soc, 10.1093/jpids/pix1059 (2017).

36. Drummond RA & Lionakis MS Candidiasis of the central nervous system in neonates and children with primary immunodeficiencies. Curr Fungal Infect Rep 12, 92–97 (2018). [PubMed: 30393511]

37. Cetinkaya PG, Ayvaz DC, Karaatmaca B, Gocmen R, Söylemezoğlu F et al. A young girl with severe cerebral fungal infection due to card 9 deficiency. Clin. Immunol. 191, 21–26 (2018). [PubMed: 29307770]

38. Lanternier F, Mahdaviani SA, Barbati E, Chaussade H, Koumar Y et al. Inherited CARD9 deficiency in otherwise healthy children and adults with *Candida* species–induced meningoencephalitis, colitis, or both. J Allergy Clin Immunol 135, 1558–1568 (2015). [PubMed: 25702837]

39. Del Rio L, Bennouna S, Salinas J & Denkers EY CXCR2 deficiency confers impaired neutrophil recruitment and increased susceptibility during Toxoplasma gondii infection. J Immunol 167, 6503–6509 (2001). [PubMed: 11714818]

40. Bonnett CR, Cornish EJ, Harmsen AG & Burritt JB Early neutrophil recruitment and aggregation in the murine lung inhibit germination of Aspergillus fumigatus conidia. Infect Immun 74, 6528–6539 (2006). [PubMed: 16920786]

41. Lévesque SA, Paré A, Mailhot B, Bellver-Landete V, Kébir H et al. Myeloid cell transmigration across the CNS vasculature triggers IL-1β-driven neuroinflammation during autoimmune encephalomyelitis in mice. J Exp Med 213, 929–949 (2016). [PubMed: 27139491]

42. Hanamsagar R, Aldrich A & Kielian T Critical role for the AIM2 inflammasome during acute CNS bacterial infection. J Neurochem 129, 704–711 (2014). [PubMed: 24484406]

43. Prinz M, Erny D & Hagemeyer N Ontogeny and homeostasis of CNS myeloid cells. Nat Immunol 18, 385–392 (2017). [PubMed: 28323268]

44. Shinozaki Y, Shibata K, Yoshida K, Shigetomi E, Gachet C et al. Transformation of astrocytes to a neuroprotective phenotype by microglia via P2Y1 receptor downregulation. Cell Rep 19, 1151–1164 (2017). [PubMed: 28494865]

45. Rothhammer V, Borucki DM, Tjon EC, Takenaka MC, Chao C-C et al. Microglial control of astrocytes in response to microbial metabolites. Nature 557, 724–728 (2018). [PubMed: 29769726]

46. Mao L, Zhang L, Li H, Chen W, Wang H et al. Pathogenic fungus Microsporum canis activates the NLRP3 inflammasome. Infect Immun 82, 882–892 (2014). [PubMed: 24478101]

47. Goodridge HS, Shimada T, Wolf AJ, Hsu Y-MS, Becker CA et al. Differential use of CARD9 by Dectin-1 in macrophages and dendritic cells. J Immunol 182, 1146–1154 (2009). [PubMed: 19124758]

48. Weinblatt ME, Kavanaugh A, Genovese MC, Musser TK, Grossbard EB et al. An oral spleen tyrosine kinase (Syk) inhibitor for rheumatoid arthritis. N Eng J Med 363, 1303–1312 (2010).

49. Flynn R, Allen JL, Luznik L, MacDonald KP, Paz K et al. Targeting Syk-activated B cells in murine and human chronic graft-versus-host disease. Blood 125, 4085–4094 (2015). [PubMed: 25852057]

Methods-only References

51. Ruland J, Duncan GS, Wakeham A, Mak TW Differential requirement for Malt1 in T and B cell antigen receptor signaling. Immunity 19(5), 749–58 (2003) [PubMed: 14614861]

52. Tay TL, Mai D, Dautzenberg J, Fernandez-Klett F, Lin G et al. A new fate mapping system reveals context-dependent random or clonal expansion of microglia. Nat Neurosci 20, 793–803 (2017) [PubMed: 28414331]

53. Goldmann T, Wieghofer P, Muller PF, Wolf Y, Varol D et al. A new type of microglia gene targeting shows TAK1 to be pivotal in CNS autoimmune inflammation. Nat Neurosci 16, 1618–1626 (2013) [PubMed: 24077561]

54. Lionakis MS, Lim JK, Lee CCR & Murphy PM Organ-specific innate immune responses in a mouse model of invasive candidiasis. J Innate Immun 3, 180–199 (2011) [PubMed: 21063074]

55. Cougnoux A, Drummond RA, Collar AL, Iben JR, Salman A et al. Microglia activation in Niemann-Pick disease, type C1 is amendableto therapeutic intervention. Hum Mol Genet 27, 2076–2089 (2018) [PubMed: 29617956]
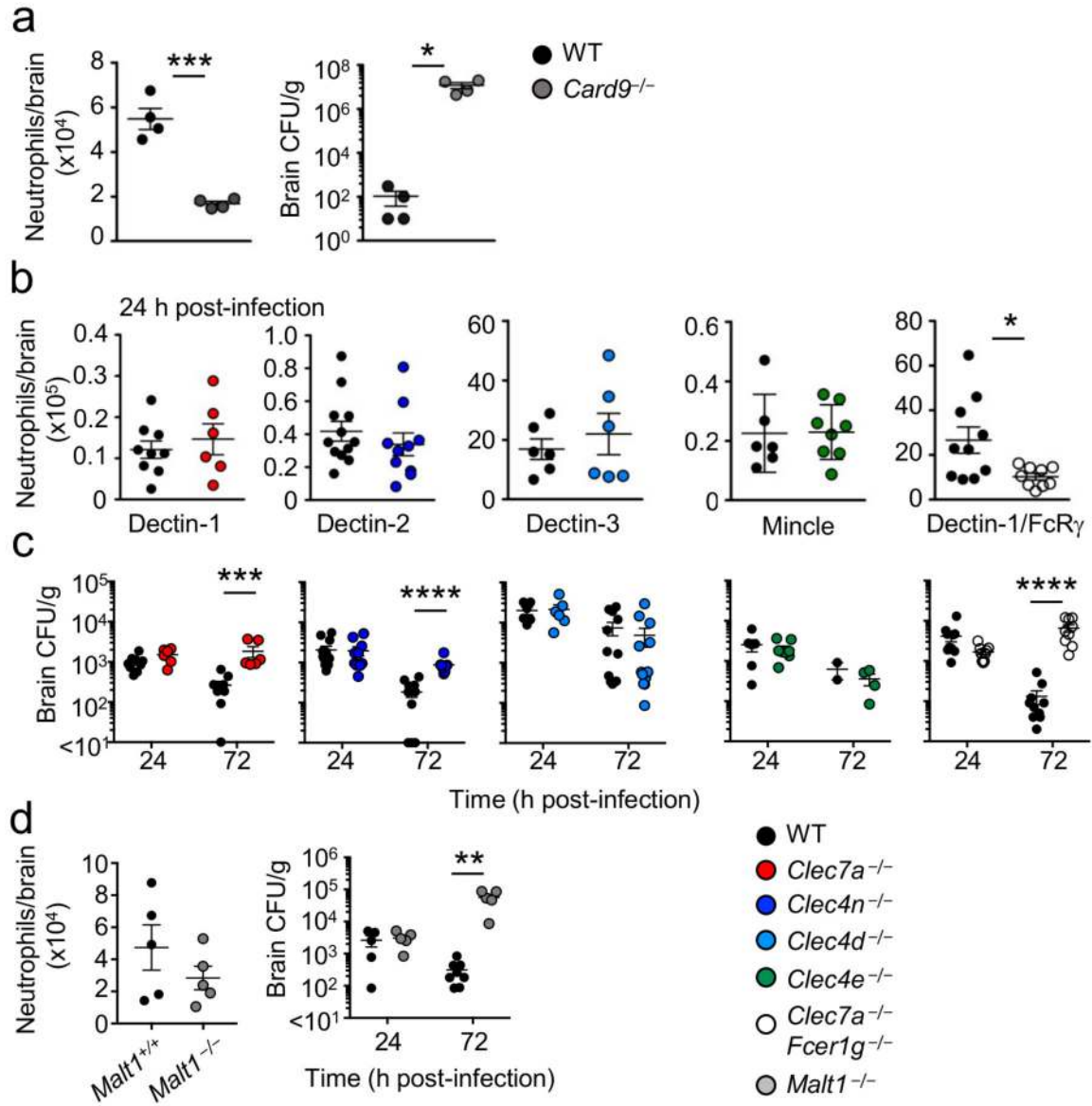
Fig. 1: Functional redundance of CARD9-coupled C-type lectin receptors for protective neutrophil recruitment to the fungal-infected brain.

a, *Card9*−/− mice (n=4 animals) and their wild-type controls (n=4 animals) were intravenously infected with *C. albicans* SC5314 and analyzed for neutrophil counts by flow cytometry at 24 h post-infection (left; dose: 1.3×10^5 CFU) and fungal growth within the brain at 72 h post-infection (right; dose: 7×10^4 CFU). **b,** Animals of the indicated genotype (WT n = 9 animals, *Clec7a*−/− n = 6 animals; WT n = 12 animals, *Clec4n*−/− n = 10 animals; WT n = 6 animals, *Clec4d*−/− n = 6 animals; WT n = 6 animals, *Clec4e*−/− n = 8 animals; WT n = 10 animals, *Clec7a*−/−*Fcer1g*−/− n = 9 animals) were intravenously infected with *C. albicans* SC5314 (2×10^5 CFU for *Clec4d*−/− and *Clec7a*−/−*Fcer1g*−/− and their controls; 1.3×10^5 all others) and analyzed for neutrophil counts by flow cytometry at 24 h post-infection and **c,** fungal burdens in the brain at 24 and 72 h post-infection (WT n = 9 animals, *Clec7a*−/− n = 6 animals; WT n = 10 animals, *Clec4n*−/− n = 10 animals; WT n = 10 animals,

Clec4d^{−/−} n = 10 animals; WT n = 6 animals, *Clec4e*^{−/−} n = 4 animals; WT n = 10 animals, *Clec7a*^{−/−}*Fcer1g*^{−/−} n = 9 animals). **d,** *Malt1*^{−/−} mice and their littermate controls were infected as above and analyzed for fungal burdens in the brain (right; WT n = 7 animals, *Malt1*^{−/−} n = 5 animals) and neutrophil recruitment to the brain at 24 h post-infection (left; WT n = 5 animals, *Malt1*^{−/−} n = 5 animals). In all cases, 'wild type' refers to appropriate matched control animals for each knock-out line for gender, age and genetic background. Individual points represent different mice. Data is pooled from 2 independent experiments and is shown as mean +/− SEM, and analyzed by unpaired two-tailed t-test (panel **a** [left], **b**) or two-tailed Mann Whitney U-test (panel **a** [right], **c**, **d**). *P<0.05, **P<0.01, ***P<0.005, ****P<0.001.
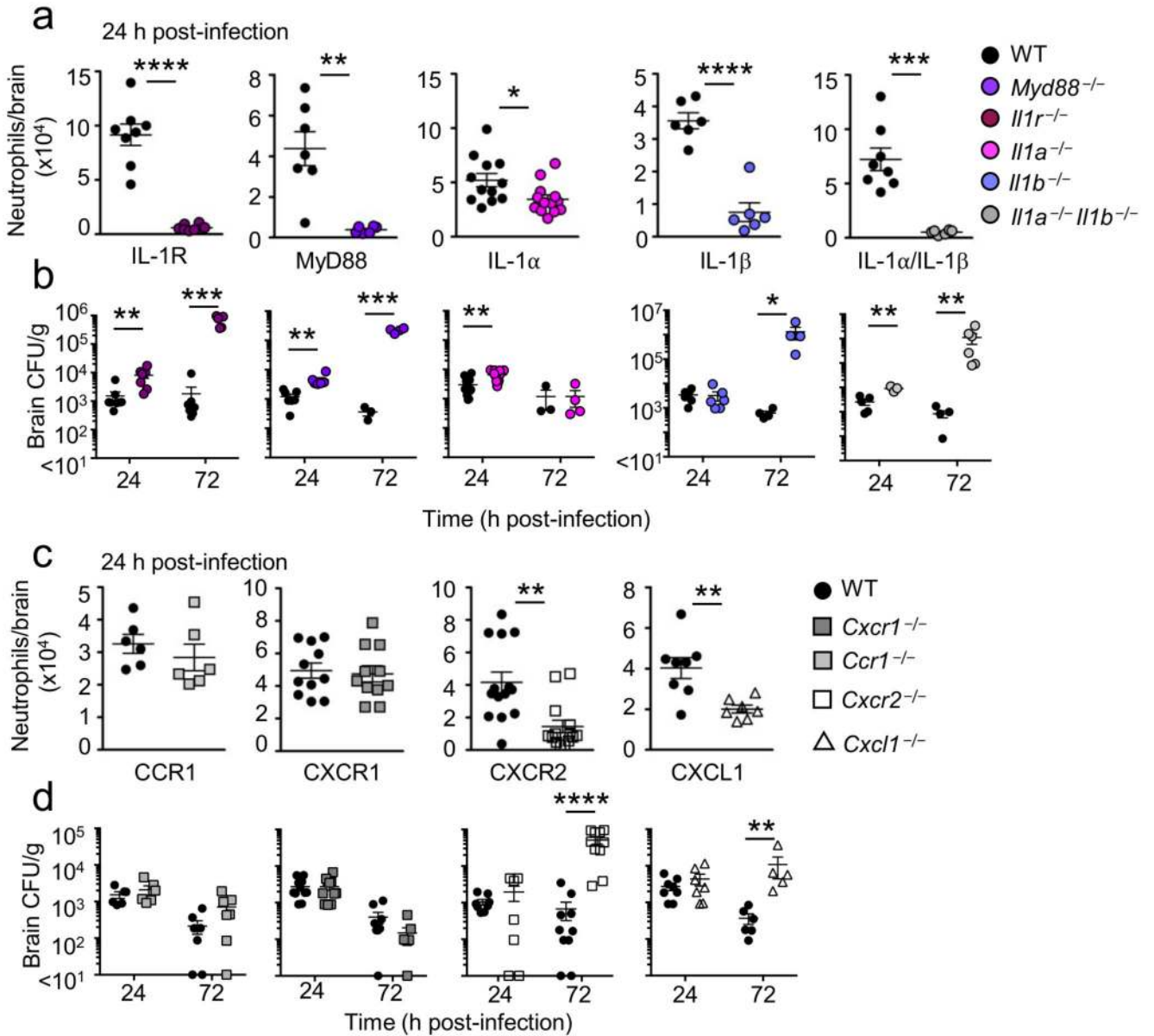
Fig. 2: IL-1β and CXCL1 mediate protective neutrophil recruitment to the fungal-infected brain.
a,b, Animals deficient in elements of the IL-1R signaling pathway or **c,d,** chemokine receptors and their ligands, were infected and analyzed for neutrophil recruitment at 24 h post-infection (**a,c**) and control of fungal brain infection (**b,d**) as in Fig. 1. 'Wild type' refers to appropriate matched control animals for each knock-out line for gender, age and genetic background. Individual points represent different mice; (**a**) WT n = 8 animals, *Il1r*^{-/-} n = 8 animals; WT n = 7 animals, *Myd88*^{-/-} n = 6 animals; WT n = 12 animals, *Il1a*^{-/-} n = 12 animals; WT n = 6 animals, *Il1b*^{-/-} n = 6 animals; WT n = 8 animals, *Il1a*^{-/-} *Il1b*^{-/-} n = 6 animals. (**b**) WT n = 8 animals, *Il1r*^{-/-} n = 7 animals; WT n = 7 animals, *Myd88*^{-/-} n = 6 animals; WT n = 3-8 animals, *Il1a*^{-/-} n = 4-8 animals; WT n = 6 animals, *Il1b*^{-/-} n = 6 animals; WT n = 6 animals, *Il1a*^{-/-} *Il1b*^{-/-} n = 6 animals. (**c**) WT n = 6 animals, *Ccr1*^{-/-} n = 6 animals; WT n = 11 animals, *Cxcr1*^{-/-} n = 11 animals; WT n = 14 animals, *Cxcr2*^{-/-} n =
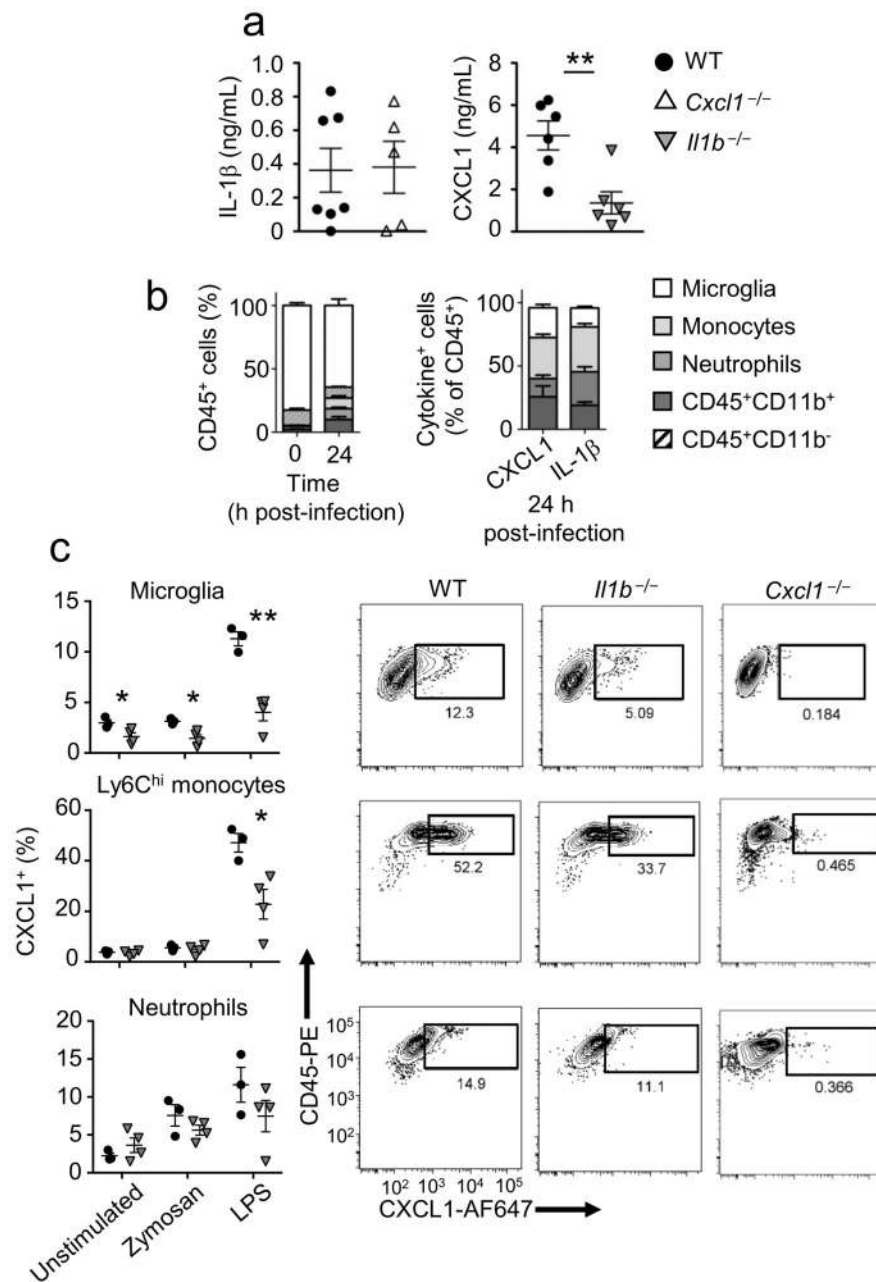
16 animals; WT n = 8 animals, $Cxcl1^{-/-}$ n = 7 animals. (**d**) WT n = 6-7 animals, $Ccr1^{-/-}$ n = 6-7 animals; WT n = 7-10 animals, $Cxcr1^{-/-}$ n = 7-10 animals; WT n = 8-10 animals, $Cxcr2^{-/-}$ n = 7-10 animals; WT n = 6-8 animals, $Cxcl1^{-/-}$ n = 5-7 animals. Data is pooled from 2-3 independent experiments and shown as mean +/− SEM, analyzed by unpaired two-tailed t-test (panel **a, c**) or two-tailed Mann Whitney U-test (panel **b, d**). *P<0.05, **P<0.01, ***P<0.005, ****P<0.001.

Fig. 3: Production of CXCL1 is dependent on IL-1β in the fungal-infected brain.

a, Wild type (n = 6/7 animals), $Cxcl1^{-/-}$ (n = 5 animals) and $Il1b^{-/-}$ (n = 6 animals) animals were infected as in Fig. 1 and brains isolated at 24 h post-infection and analyzed for CXCL1 or IL-1β production by ELISA. Data is pooled from 2 independent experiments and analyzed by unpaired two-tailed t-test. **b**, The relative proportions of myeloid cell populations (gated within live CD45$^+$ singlets) in the uninfected (n = 6 animals) and 24 h infected WT (n = 6 animals) brain (left), and the relative proportion of myeloid cell populations producing CXCL1 (n = 3 animals) or pro-IL-1β (n = 9 animals) in the 24 h infected brain (right). For the latter, total CD45$^+$CXCL1(or IL-1β)$^+$ cells were first gated and then cell types defined within this initial gate using lineage markers (see below), using

samples from the unstimulated condition. Data is shown as the mean +/− SEM. **c,** Wild type (n = 3 animals) and $Il1b^{-/-}$ mice (n = 4 animals) were infected with 2×10^5 *C. albicans* and brain cells analyzed for CXCL1 production by intracellular flow cytometry 24 h later. Brain cells were restimulated *ex vivo* with 62.5 μg/mL depleted zymosan or 1 μg/mL LPS for 4 h in the presence of 5 μg/mL Brefeldin A. Representative plots from the LPS-stimulated condition are gated on microglia (top; CD45^{int} Ly6G$^-$ CD11b$^+$), Ly6C^{hi} monocytes (middle; CD45^{hi} Ly6C^{hi} Ly6G$^-$ CD11b$^+$) and neutrophils (bottom; CD45^{hi} Ly6C^{int} Ly6G^{hi} CD11b$^+$), showing corresponding $Cxcl1^{-/-}$ cells as gating controls. In all panels, 'wild type' refers to appropriate matched control animals for each knock-out line for gender, age and genetic background. Individual points represent different mice. Data shown as mean +/− SEM, and analyzed by unpaired two-tailed t-test. *P<0.05, **P<0.01.
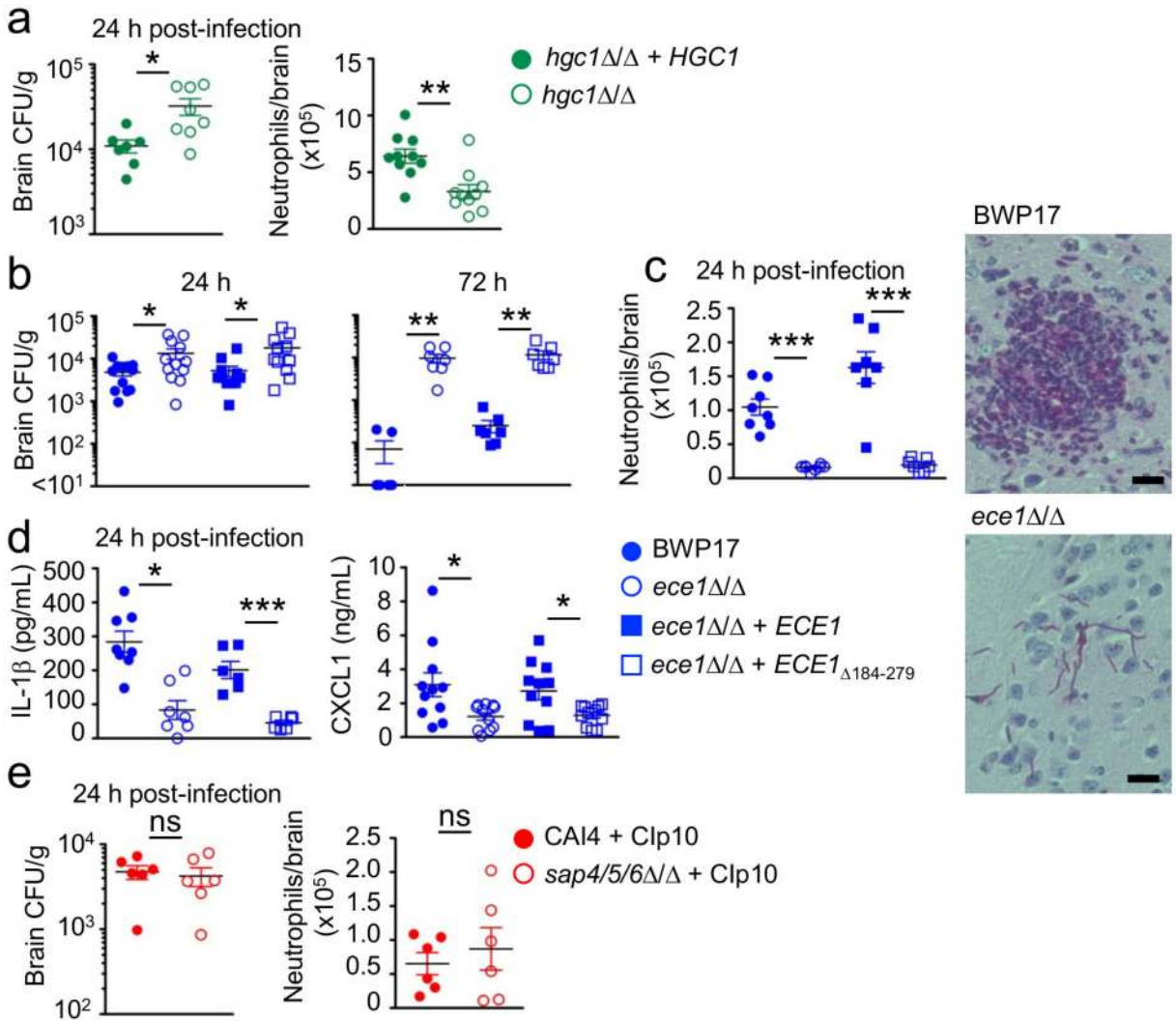
Fig. 4: Fungal-derived Candidalysin promotes neutrophil recruitment and control of fungal growth in the brain.

a,b,c,e, Animals were infected with 2×10^5 CFU of the indicated *C. albicans* strains (parental strains, closed symbols; deficient mutants, open symbols) and analyzed as in Fig. 1 for fungal burdens (*hgc1Δ/Δ* n = 8 animals, *hgc1Δ/Δ + HGC1* n = 7 animals; BWP17 n = 10 animals, *ece1Δ/Δ* n = 11 animals, *ece1Δ/Δ + ECE1* n = 10 animals, *ece1Δ/Δ + ECE1*$_{Δ184-279}$ n = 11 animals; CAI4 + CIp10 n = 6 animals, *sap4/5/6Δ/Δ* + CIp10 n = 6 animals) and neutrophil recruitment (*hgc1Δ/Δ* n = 10 animals, *hgc1Δ/Δ + HGC1* n = 10 animals; BWP17 n = 7 animals, *ece1Δ/Δ* n = 7 animals, *ece1Δ/Δ + ECE1* n = 7 animals, *ece1Δ/Δ + ECE1*$_{Δ184-279}$ n = 11 animals; CAI4 + CIp10 n = 6 animals, *sap4/5/6Δ/Δ* + CIp10 n = 7 animals). Histology shown in **(c)** is from 24 h post-infection, stained with PAS. Scale bar is 50 μm. **d,** Whole brain homogenates from animals infected with indicated strains were isolated at 24 h post-infection and analyzed for IL-1β and CXCL1 using ELISA (BWP17 n = 8-10 animals, *ece1Δ/Δ* n = 8-10 animals, *ece1Δ/Δ + ECE1* n = 6-11 animals, *ece1Δ/Δ + ECE1*$_{Δ184-279}$ n = 7-11 animals). Individual points represent different mice. Data is pooled from 2-4 independent experiments and shown as mean +/− SEM, analyzed by unpaired two-
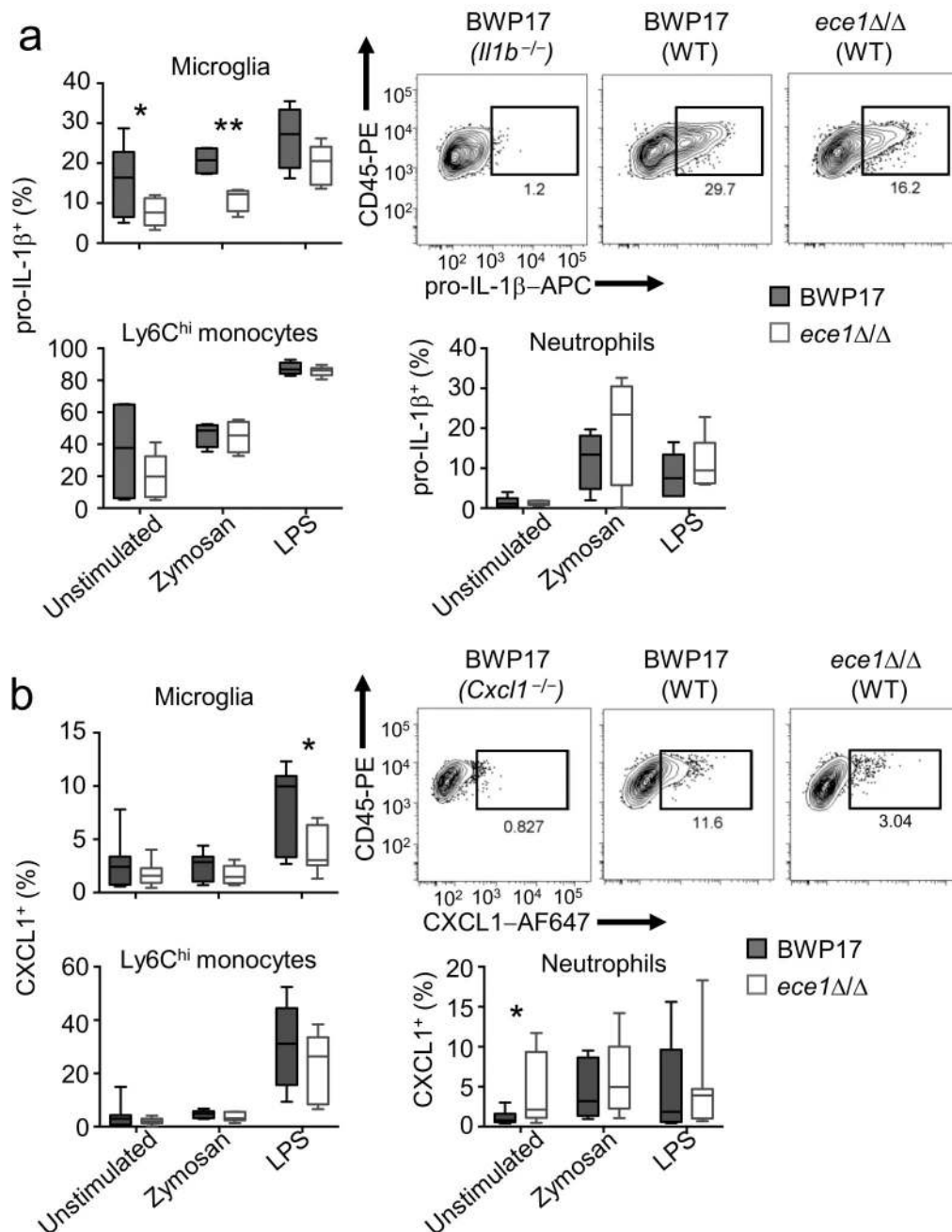
tailed t-test, or two-tailed Mann Whitney U-test (panel **a**, left). *P<0.05, **P<0.01, ***P<0.005; ns = not significant.

Fig. 5: Microglia produce IL-1β and CXCL1 in a Candidalysin-dependent manner.
Animals were infected with wild-type *C. albicans* (BWP17; closed bars) or a Candidalysin-null strain (*ece1Δ/Δ*; open bars), and brain cells isolated 24 h later. Brain leukocytes were restimulated as in Fig. 3, and intracellular staining for **a,** IL-1β (unstimulated, n = 8 animals; zymosan, n = 4 animals; LPS n = 6 animals) and **b,** CXCL1 (unstimulated, n = 12 animals; zymosan, n = 6 animals; LPS n = 9 animals) was analyzed by flow cytometry. Box-and-whisker plots show the minimum/maximum values (whiskers), the 25th/75th percentiles and the median. Data is pooled from 2-4 independent experiments and analyzed by unpaired two-tailed t-tests. *P<0.05, **P<0.01. Representative staining is shown for LPS-stimulated
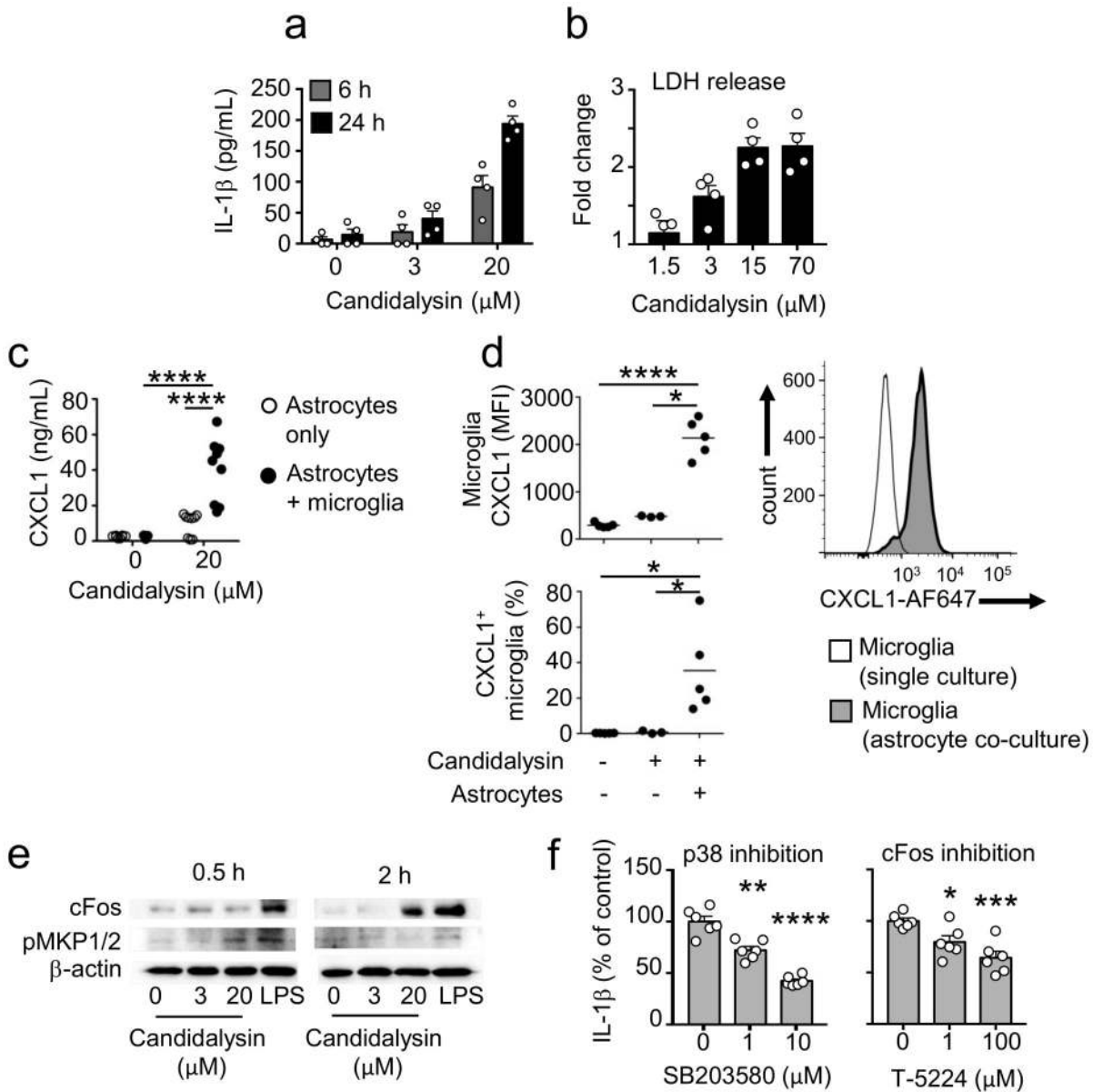
microglia (gated as in Fig. 3) from wild-type mice infected with indicated strains, or BWP17-infected cytokine-deficient mutants as control.

Fig. 6: Candidalysin activates microglial IL-1β production via p38-cFos signaling and promotes microglial CXCL1 production through astrocyte interactions.
BV-2 microglia were seeded into 24-well plates at 5×10^5 per well and left to adhere for 2 h in the presence of 50 n g/mL LPS (for priming) before the addition of purified Candidalysin at the indicated concentrations. Cell culture supernatants were analyzed for **a,** IL-1β production or **b,** LDH release after 24 h of stimulation. Data is shown with the mean +/− SEM, individual points represent individual culture wells (n = 4). **c-d,** In some experiments, BV-2 cells were co-cultured with 3×10^5 C8-D1A astrocytes, and CXCL1 production analyzed in the supernatant by ELISA (n = 10 individual culture wells) or by intracellular flow cytometry (n = 3-5 individual culture wells; data shown with the mean). In **d**, microglia and astrocytes were distinguished by CD45 staining, and CXCL1 production assessed within CD45^{+} (microglia) and CD45^{−} (astrocyte) gates. Histogram is gated on CD45^{+} microglia. **e,**

To measure cFos and pMKP½ activation, BV-2 cells were stimulated with the indicated Candidalysin concentrations for 30 or 120 min and BV-2 cells then lysed and analyzed for cFos and pMKP½ by immunoblot, normalizing to β-actin. Immunoblots shown are representative of 2 independent experiments. **f,** BV-2 cells were cultured in the presence of the indicated cFos and p38 inhibitors for 2 h prior to stimulating with 20 μM Candidalysin, and IL-1β measured in the supernatant by ELISA after 24 h (data shown as mean +/− SEM; n = 6 individual culture wells). All data is pooled from 2 independent experiments and analyzed by one-way ANOVA. *$P<0.05$, **$P<0.01$, ***$P<0.005$, ****$P<0.0001$.
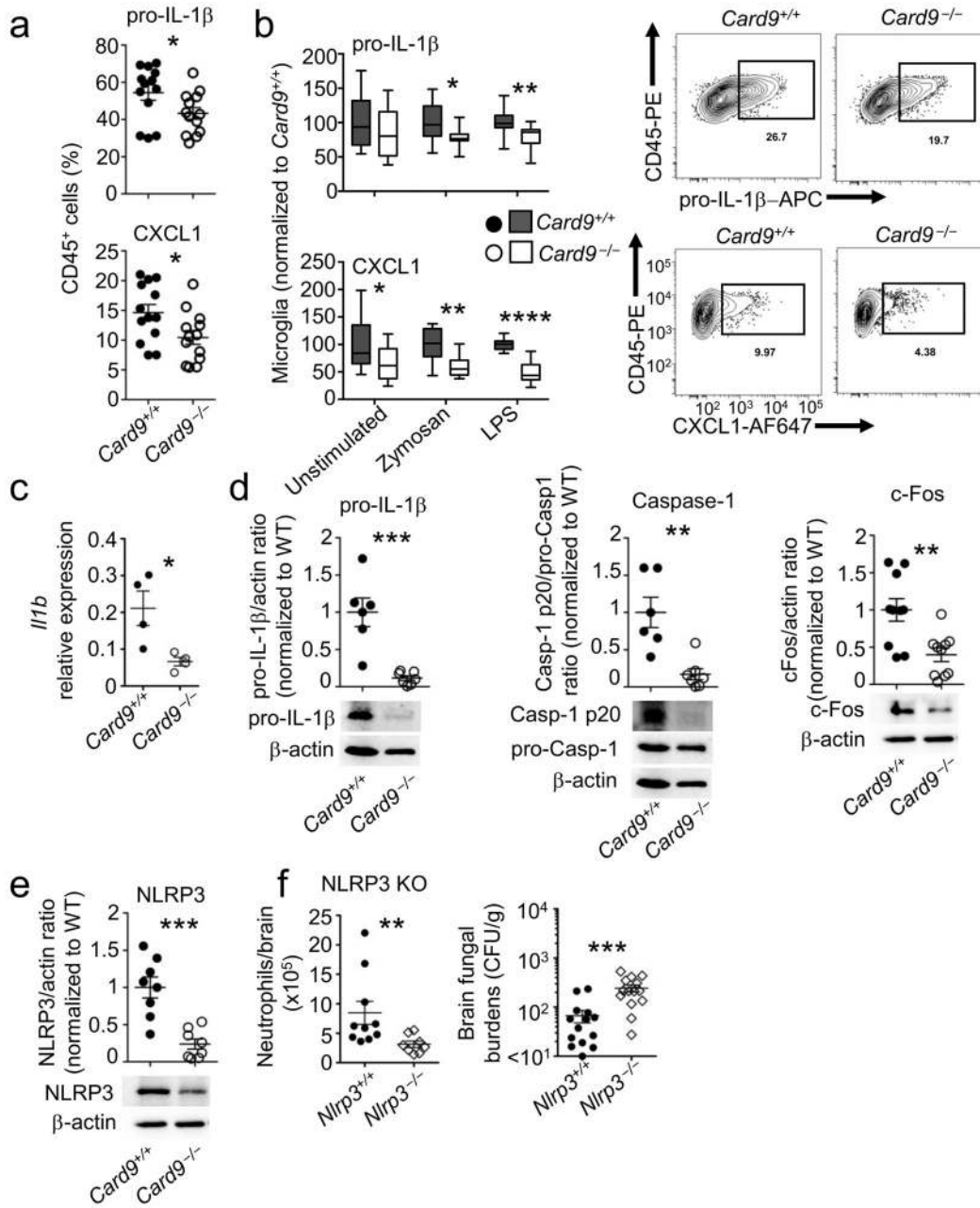
Fig. 7: CARD9 is required for microglial pro-IL-1β transcription, inflammasome activation, and CXCL1 production in the fungal-infected brain.

a,b, *Card9+/+* (n = 13 animals) and *Card9−/−* (n = 13 animals) animals were infected with 2 × 10^5 CFU wild-type *C. albicans* (BWP17), and brain cells isolated 24 h later. Brain leukocytes were restimulated as in Fig. 4, and intracellular staining for pro-IL-1β and CXCL1 analyzed by flow cytometry in total CD45+ cells (LPS-stimulated condition shown) (**a**) or microglia alone, normalized to *Card9+/+* results (**b**). Panels **a,b** show pooled data from 4 independent experiments, analyzed with two-tailed unpaired t-test. Data shown as mean +/− SEM (**a**) or with minimum/maximum values (whiskers), the 25th/75th percentiles and the median (**b**). **c,** Microglia were FACS-sorted from pooled *Card9+/+* (n = 4 animals) and

Card9⁻/⁻ animals (n = 4 animals) at 24 h post-infection and analyzed by unpaired two-tailed t-test for *Il1b* expression by qRT-PCR, or **d,e,** the indicated proteins by immunoblot (Caspase and IL-1β blots; WT n = 6 animals, *Card9⁻/⁻* n = 7 animals; cFos blot; WT n = 10 animals, *Card9⁻/⁻* n = 10 animals; NLRP3 blot; WT n = 8 animals, *Card9⁻/⁻* n = 8 animals;). Graphs in (**d,e**) represent the band pixel density normalized to the wild type control, and are shown with mean +/− SEM and analyzed by unpaired two-tailed student t-tests. Example blots are representative of 3 independent FACS sorts/experiments; pooled data is shown in the graphs above. **f,** *Nlrp3⁻/⁻* animals and their wild-type controls were infected with 1.3×10^5 CFU *C. albicans* and analyzed by unpaired two-tailed t-tests for neutrophil recruitment to the brain 24 h later (left; WT n = 9 animals, *Nlrp3⁻/⁻* n = 8 animals) and by two-tailed Mann-Whitney U-test for fungal brain burdens at 72 h post-infection (right; WT n = 14 animals, *Nlrp3⁻/⁻* n = 14 animals), as described in Fig. 1. *$P<0.05$, **$P<0.01$, ***$P<0.005$.
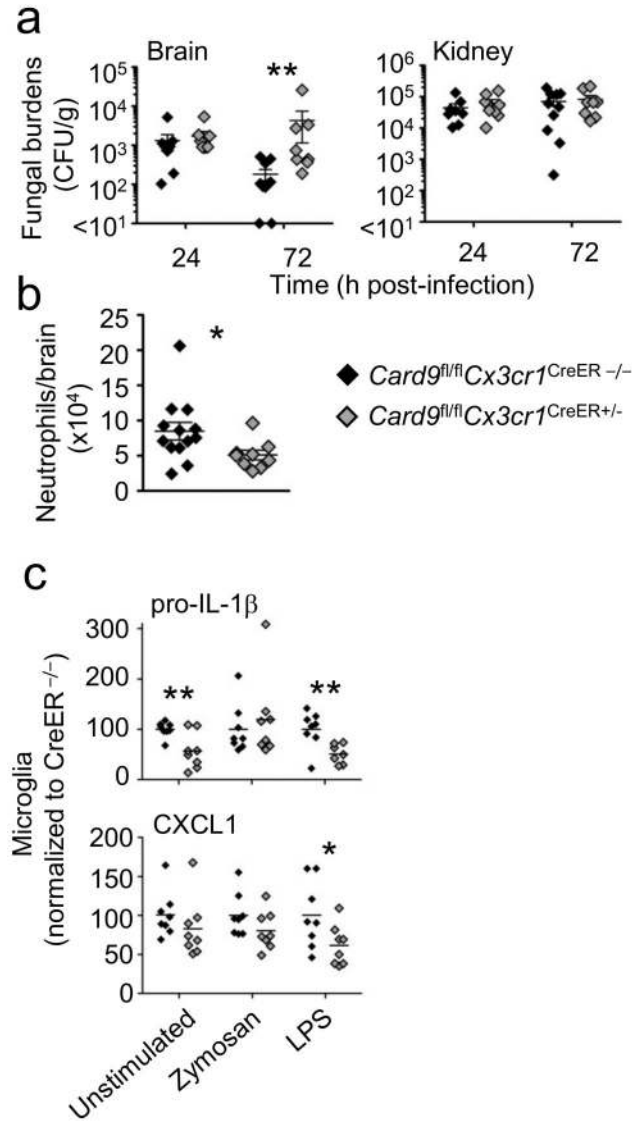
Fig. 8: CARD9 is required specifically in microglia for neutrophil recruitment and control of fungal invasion in the CNS.

a, $Card9^{fl/fl}Cx3cr1^{CreER-/-}$ and $Card9^{fl/fl}Cx3cr1^{CreER+/-}$ littermates (n=8-13) were tamoxifen-pulsed at 4-5 weeks of age, left to rest for 4-6 weeks and then infected with 1.3×10^5 CFU *C. albicans* (SC5314) intravenously and analyzed for brain and kidney fungal burdens ($Card9^{fl/fl}Cx3cr1^{CreER-/-}$ n = 8-10 animals; $Card9^{fl/fl}Cx3cr1^{CreER+/-}$ n = 8 animals), **b,** neutrophil recruitment to the brain at 24 h post-infection ($Card9^{fl/fl}Cx3cr1^{CreER-/-}$ n = 13 animals; $Card9^{fl/fl}Cx3cr1^{CreER+/-}$ n = 9 animals), and **c,** intracellular staining for pro-IL-1β and CXCL1, as described in Fig. 3 ($Card9^{fl/fl}Cx3cr1^{CreER-/-}$ n = 8 animals; $Card9^{fl/fl}Cx3cr1^{CreER+/-}$ n = 8 animals). Data is pooled from 2-4 independent experiments and is shown as mean +/− SEM, analyzed by two-tailed Mann-Whitney U-tests (panel **a**) or two-tailed unpaired t-tests (panel **b, c**). *P<0.05, **P<0.01.